RSC Advances

PAPER

View Article Online
View Journal | View Issue

Cite this: *RSC Adv.*, 2018, **8**, 18372

A novel application of electrospun silk fibroin/poly(L-lactic acid-*co*-ε-caprolactone) scaffolds for conjunctiva reconstruction

Qinke Yao,†[ab] Yang Hu,†[ab] Fei Yu,[ab] Weijie Zhang[ab] and Yao Fu *[ab]

Electrospun hybrid nanofibers prepared using combinations of natural and synthetic polymers have been widely investigated in tissue engineering. In this study, silk fibroin (SF) and poly(L-lactic acid-*co*-ε-caprolactone) (PLCL) hybrid scaffolds were successfully prepared by electrospinning. Scanning electron micrographs (SEM) showed that SF/PLCL scaffolds were composed of defect-free nanofibers with a smooth and homogeneous fiber morphology. Water contact angle measurements demonstrated that the scaffolds were hydrophilic. To assess the cell affinity of SF/PLCL scaffolds, rabbit conjunctival epithelial cells (rCjECs) were cultured on the electrospun scaffolds. Scanning electron micrographs and *in vitro* proliferation assays showed that the cells adhered and proliferated well on the scaffolds. The quantitative polymerase chain reaction (qPCR) results showed excellent expression of CjEC genes, with reduced expression of inflammatory mediators. Hematoxylin and eosin (H&E) staining showed that the engineered conjunctiva constructed with SF/PLCL scaffolds consisted of 2–4 layers of epithelium. Furthermore, SF/PLCL scaffolds transplanted subcutaneously exhibited excellent biocompatibility. Therefore, SF/PLCL scaffolds may find biomedical applications in conjunctival reconstruction in the near future.

Received 21st December 2017
Accepted 8th May 2018

DOI: 10.1039/c7ra13551c

rsc.li/rsc-advances

Introduction

The conjunctival epithelium and corneal epithelium form the outer surface of the eye, and injury to one part may result in system-wide secondary dysfunction.[1] The conjunctival epithelium, covering the ocular surface from the limbus to the posterior surface of the eyelids, is composed of a stratified non-keratinized epithelium with goblet cells, which are specialized epithelial cells.[2,3] Normal function of the conjunctiva is crucial for the integrity of the ocular surface as it can provide the mucin component of the tear film, and serve as a barrier against external stimuli.[4,5] Therefore, ocular surface reconstruction almost inevitably fails unless the conjunctival surface is first repaired and a deep fornix is restored. Although the conjunctiva has the capacity to spontaneously re-epithelialize upon injury, this is usually accompanied by a certain amount of fibrosis and wound contracture, especially in extensive disorders such as chemical/thermal burns, Stevens–Johnson syndrome, microbial infection, and ocular cicatricial pemphigoid.[6–8] In these cases, tissue engineering needs to be applied for conjunctival reconstruction.

The general principle of tissue engineering is to repair or generate the damaged tissue using three-dimensional scaffolds, in combination with cells and/or growth factors to rapidly heal damaged tissue.[9] The scaffolds should be biocompatible and have similar properties to the native extracellular matrix (ECM).[10] Moreover, for each specific tissue, a scaffold should have suitable mechanical properties, a well-interconnected pore network, and an optimum pore size.[11] Among the currently known fabrication techniques, electrospinning has been shown to be an effective approach for producing nanofibrous scaffolds that facilitate cell adhesion and proliferation, and allow for an efficient exchange of nutrients and metabolites.[12,13]

SF, a kind of natural protein, has been widely used in a number of biomedical applications due to its unique properties including good biocompatibility, low toxicity, and lower pro-inflammatory effects compared to collagen.[14–16] However, scaffolds made of SF alone failed to fulfil the desired mechanical characteristics, as in previous reports which showed that the pure SF nanofibrous scaffolds typically underwent brittle fracture.[12] PLCL, a copolymer of L-lactic acid and PCL, is one of the most common polymers for tissue engineering due to its good mechanical properties and tunable biodegradability, but having no natural cell recognition sites greatly limits its application in the biomedical field.[17–19] Therefore, the blending of bioactive SF with the beneficial mechanical properties of PLCL will produce a new biohybrid material which may be suitable for conjunctival reconstruction. In previous studies, we have

[a]*Department of Ophthalmology, Ninth People's Hospital, Shanghai Jiao Tong University School of Medicine, 639 Zhizaoju Road, Shanghai 200011, China. E-mail: drfuyaofy@sina.com; Fax: +86 021 6313 7148; Tel: +86 021 6313 5606*

[b]*Shanghai Key Laboratory of Orbital Diseases and Ocular Oncology, Shanghai, China*

† These authors contributed equally to this work.

applied SF/PLCL scaffolds for corneal endothelial reconstruction, retinal reconstruction and bone regeneration.[20–22]

In this study, we attempted to employ SF/PLCL scaffolds to engineer a conjunctival equivalent. Systematic experiments were conducted to evaluate the physiochemical properties of the SF/PLCL scaffolds, and we explored the effects of SF/PLCL scaffolds on cell adhesion, viability, proliferation, inflammatory reaction and cell stratification. Based on these evaluations, we present a promising scaffold with favorable mechanical and biological properties for conjunctival regeneration.

Experimental

Materials

Cocoons of *Bombyx mori* silkworms were kindly supplied by Jiaxing Silk (China). A copolymer of PLCL, which has a composition of 50 mol% L-lactide, was used. 1,1,1,3,3,3-Hexafluoro-2-propanol (HFIP) was purchased from Daikin Industries (Japan).

SF/PLCL nanofibrous scaffold preparation

Composite fibers of SF/PLCL scaffolds were fabricated as described previously.[12,21] Briefly, raw silk was degummed three times using a 0.5 wt% (0.02 M) Na_2CO_3 (Sigma-Aldrich Co., St Louis, MO, USA) solution at 100 °C for 30 min each time and it was washed with sterilized distilled water three times. Then degummed silk was dissolved in a ternary solvent system of $CaCl_2/H_2O$/ethanol (mole ratio 1/8/2) for 1 h at 70 °C. The SF solution was dialyzed through a cellulose tubular membrane with a pore size of about 250–257 μm in distilled water for 3 days at room temperature, then filtered and lyophilized to obtain regenerated SF sponges. After PLCL and SF were dissolved in 1,1,1,3,3,3-hexafluoro-2-propanol with 8 w/v % concentrations, they were then mixed in a 1 : 3 volume ratio by stirring at room temperature for 1 h. The electrospinning conditions were as follows: 1.2 mL h^{-1} injection rate, 12 kV voltage and 12–15 cm distance. SF/PLCL scaffolds were dried in a fume cupboard at room temperature and stored in desiccators. SF/PLCL scaffolds were sterilized under an ultraviolet lamp for 30 min at room temperature before being placed into 24-well culture plates.

Characterization of SF/PLCL scaffolds

Scanning electron microscopy (SEM). The surface microstructure of SF/PLCL scaffolds was characterized using scanning electron microscopy (SEM; JSM-6701, JEOL, Japan). The average diameter of electrospun nanofibers was measured using image analysis software (Image Pro Plus 6.0, Rockville, MD, USA) and calculated by selecting at least 50 nanofibers randomly as observed on the SEM images.

Contact angle measurements. Surface wettability of SF/PLCL scaffolds was characterized by water contact angle measurements, as previously reported.[23] The contact angle was visualized by a video contact angle instrument (Attension Theta, Finland). Deionized water was used as the testing liquid. Droplets were set at a 0.8 μL size and dropped onto the surface of the scaffolds. Each experiment was duplicated three times in different positions.

Mechanical measurements. The tensile modulus of the SF/PLCL scaffolds was measured using a materials testing machine (Instron 5542, MA, USA) under a crosshead speed of 10 mm min^{-1} and a load cell of 10 N. All specimens from the scaffolds were prepared in a rectangular shape with dimensions of 10 × 30 mm. Scaffolds with thicknesses of 20–30 μm were used for testing. At least five samples were tested.

Isolation and culture of conjunctival epithelial cells

Cell isolation and culture were performed as previously described.[24] Briefly, the conjunctiva was obtained from the palpebral conjunctiva containing the fornix of New Zealand white rabbits (about 2 months in age, 2–3 kg, $n = 30$), with the underlying connective tissue removed. The conjunctiva tissue was rinsed three times with phosphate-buffered saline (PBS) containing 100 U mL^{-1} penicillin, then incubated in Dispase II (2.4 units per mL; Sigma-Aldrich, St. Louis, MO, USA) at 4 °C for 16 h. The detached epithelium layer was scattered into single cells by incubation with 0.05% trypsin/EDTA (Gibco) for 10 min at 37 °C. Then, DMEM/F-12 (1 : 1; Invitrogen, Carlsbad, CA) supplemented with 10% (v/v) FBS (HyClone Laboratories, Inc., Logan, UT), 5 μg mL^{-1} insulin, 5 μg mL^{-1} transferrin, 5 ng mL^{-1} selenium, 1% penicillin/streptomycin, 10 ng mL^{-1} human epidermal growth factor (hEGF; R&D Systems), and 100 ng mL^{-1} nerve growth factor (NGF; R&D Systems) were added as the culture medium and the cells were seeded on a cell culture dish (Millipore Corporation, Billerica, MA). When 80–90% confluence was reached, the cells were passaged. Passage one of the cells was used for further experiments. All animal procedures were performed in accordance with the Guidelines for Care and Use of Laboratory Animals of Shanghai Jiao Tong University School of Medicine and approved by the Animal Ethics Committee of the Ninth People's Hospital affiliated to Shanghai Jiao Tong University, School of Medicine.

Characterization of conjunctival epithelial cells on SF/PLCL scaffolds

Morphology of conjunctival epithelial cells cultured on SF/PLCL scaffolds. CjECs were seeded onto SF/PLCL scaffolds at a density of 20 × 10^5 cells per well in 24-well plates. Two days after seeding, the samples were fixed with 0.25% glutaraldehyde overnight at 4 °C, rinsed three times in PBS, and then dehydrated with graded concentrations (50, 70, 80, 90, 95 and 100% volume ratios) of ethanol for 10 min each. Subsequently, the samples were critical-point dried overnight, coated with gold sputter and then observed by SEM.

Cell phenotypes. Cell phenotypes were confirmed by assessment of the expression of CK4, CK19, and MUC5AC.[24] Briefly, the cell-seeded scaffolds were fixed with 4% w/v PFA for 30 min at room temperature. The samples were incubated overnight in the primary antibodies (CK4, CK19, and MUC5AC). Fluorescent-labeled secondary antibodies (Alexa Fluor 488 goat anti-rabbit/mouse antibodies) were used for detection of CK4, CK19, and MUC5AC. After washing, nuclei were counterstained with Hoechst 33342. Images were taken under a confocal laser

scanning microscope (Carl Zeiss Microscopy, Oberkochen, Germany).

Cell proliferation. Cell proliferation was examined using a Cell Counting Kit-8 (CCK-8, Dojindo, Kumamoto, Japan) and BrdU staining. The CCK-8 assay was carried out according to the manufacturer's instructions (Dojindo Molecular Technologies, Inc., Tokyo, Japan), as previously reported. CjECs were seeded onto SF/PLCL scaffolds at a density of 2×10^4 cells per well in 48-well plates. After 0, 1, 3, 5 and 7 days, 10 μL of the CCK-8 solution was added to each well. After incubation for 3 h, the supernatant was pipetted into a new 96-well plate. The absorbance at 450 nm for each well was measured using a microplate reader (Multiskan MK3, Thermo Electron Corporation, MA, USA). At least six samples were measured at each time point. All experiments were performed in triplicate. BrdU staining was carried out using standard procedures as described previously.[22] CjECs were seeded onto the scaffolds in 24-well plates at a density of 20×10^4 cells per well. When 70–80% confluence was reached, the medium was replaced with fresh culture medium containing 10 μM BrdU for 4 h, then the samples were fixed in 4% w/v PFA for 15 min at room temperature and blocked for 1 h in a blocking solution. The samples were washed with PBS and incubated with 1 N HCl for 30 min, followed by several rinses in Hank's Balanced Salt Solution (HBSS) and PBS. After overnight incubation at 4 °C with anti-BrdU antibodies (1 : 250, Santa Cruz Biotechnology, Santa Cruz, CA), they were washed in PBS, and fluorescent-labeled secondary antibodies (Alexa Fluor 488 goat anti-rabbit/mouse antibodies; Life Technologies) were diluted 1 : 800 in PBS and applied for 1 h at room temperature. After washing, cell nuclei were counterstained with Hoechst 33342 (Invitrogen). We did not add the primary antibody and only added the secondary antibodies in the negative control groups. Images were taken under a confocal laser scanning microscope (Carl Zeiss Microscopy, Oberkochen, Germany).

Cell viability. The Live/Dead Viability/Cytotoxicity Assay Kit (Invitrogen, Carlsbad, CA) was used to distinguish viable cells from dead cells, and this is based on the differential permeability of live and dead cells.[25] In brief, CjECs cultured on the scaffolds were incubated in PBS containing 2 mM calcein acetoxymethyl ester and 2 mM ethidium homodimer-1 (Invitrogen) for 30 min at 37 °C and then observed under a fluorescence microscope (Olympus BX51, Japan).

Gene expression detection of cell-seeded scaffolds

The cell-seeded scaffolds were removed from coverslips using microscope forceps and ground using a Micro Tissue Grinder (PRO Scientific Inc., Oxford, CT, USA). Total RNA was extracted using the Trizol reagent (Life Technologies, USA). Free DNase I was used to remove any contaminating genomic DNA. The RNA concentration was measured using a NanoDrop ND-2000 spectrophotometer (Thermo Fisher Scientific Inc., USA). cDNA was synthesized using a high capacity reverse transcription kit for the quantitative polymerase chain reaction (qPCR) (Life Technologies). qPCR was performed using specific primers (Table 1) to analyze the expression levels of CjEC-marker genes and pro-inflammatory genes. Each sample was tested in triplicate. The relative gene expressions were analyzed using the Pfaffl method.[26] The relative mRNA levels were expressed as the fold change relative to the cells cultured on the tissue culture polystyrene surface (TCPS) after being normalized to the expression of glyceraldehyde-3-phosphate dehydrogenase (GAPDH). It is commonly accepted that TCPS provides a hydrophilic surface for cell adhesion, therefore, cells grown on TCPS were used as the positive control.

In vivo implantation

Six nude mice for each experiment were supplied by the Shanghai Animal Experimental Center, and all animal procedures were performed in accordance with the Guidelines for Care and Use of Laboratory Animals of Shanghai Jiao Tong University School of Medicine and approved by the Animal Ethics Committee of the Ninth People's Hospital affiliated to Shanghai Jiao Tong University School of Medicine. SF/PLCL scaffolds were tailored into a round shape (10 mm diameter) and sterilized, and then placed in the bottom of a 24-well culture plate with 100 μL of cell suspension at 1×10^8 cells per mL. After 3 days of culturing *in vitro*, the cell-seeded scaffolds were implanted into the nude mice subcutaneously. After implantation for 1, 2, and 4 weeks, respectively, the nude mice were sacrificed and the samples were collected for further experiments. Each experiment was tested in triplicate.

Histology and immunohistochemistry

H&E staining was performed on both *in vitro* and *in vivo* samples as previously described.[27] Briefly, *in vitro* and *in vivo* cell-seeded scaffolds were embedded in Tissue-Tek OCT compound (Sakura Seiki, Tokyo, Japan), quickly frozen and cut into 10 mm-thick sections. After being dried for 30 min at room temperature, the sections were fixed with 4% w/v PFA at room temperature for 15 min, then washed three times with distilled-deionized water (DDW) and stained with H&E. Microphotographs were taken with a light microscope (Olympus BX51, Japan). For the immunochemistry, primary antibodies of MUC5AC were used to stain the sections. The secondary antibody was used to visualized the specific antigen.

Table 1 Primers used in qPCR studies

Genes	Accession number	Forward (5′–3′)	Reverse (5′–3′)	Annealing temperature (°C)	Product size (base pairs)
CK4	XM_008256495.1	CAACCTGAAGACCACCAAGA	CAGAGTCTGGCACTGCTTT	60	100
MUC5AC	XM_008253634.1	TGATGACCAACCAGGTCATTT	GGGATGGTCACGTACATCTTG	60	106
GAPDH	NM_001082253	GGTCGGAGTGAACGGATTT	TGTAGTGGAGGTCAATGAATGG	60	113
IL-6	NM_001082064.2	TGTACGATCACTGAACTGCA	GAAGTCAGTTATATCCTGGC	60	291

Statistical analysis

All of the data presented in this paper are shown as mean ± standard deviation (SD). All experiments were performed with at least three repeats. Analysis of variance followed by Student's *t* test was used to determine significant differences between the control and the test groups. A value of $p < 0.05$ was considered statistically significant.

Results

Physicochemical properties of SF/PLCL scaffolds

The scaffolds demonstrated transparency following immersion in cell culture media (Fig. 1A). The tensile modulus was used to confirm the operability of the scaffolds. As shown in Fig. 1B, the average tensile modulus of the scaffolds was 16.53 ± 2.43 MPa.

The assessment of the surface wettability using the video contact angle instrument is presented in Fig. 1C. We observed that the water drop was absorbed into SF/PLCL scaffolds, reducing by 35.2° after 7 seconds, indicating that SF/PLCL scaffolds were hydrophilic and suitable for cell seeding.

The scanning electron micrographs of SF/PLCL scaffolds showed that the scaffolds consisted of randomly distributed, uniform, smooth nanofibers and the average nanofiber diameter of SF/PLCL scaffolds was 215 ± 69 nm (Fig. 1D).

Characterization of conjunctival epithelial cells on SF/PLCL scaffolds

SEM was used to observe cell morphology and the adhesion between the cells and scaffolds. As shown in Fig. 2A, the cells strongly adhered and exhibited a polygonal shape with lamellipodia on the scaffolds after culturing for 2 days. Epithelial cells and goblet cells can be identified by the presence of CK4 (Fig. 2B), CK19 (Fig. 2C) and MUC5AC (Fig. 2D). qPCR was conducted to characterize the gene expression of conjunctival epithelial cells. Cells cultured on SF/PLCL scaffolds exhibited

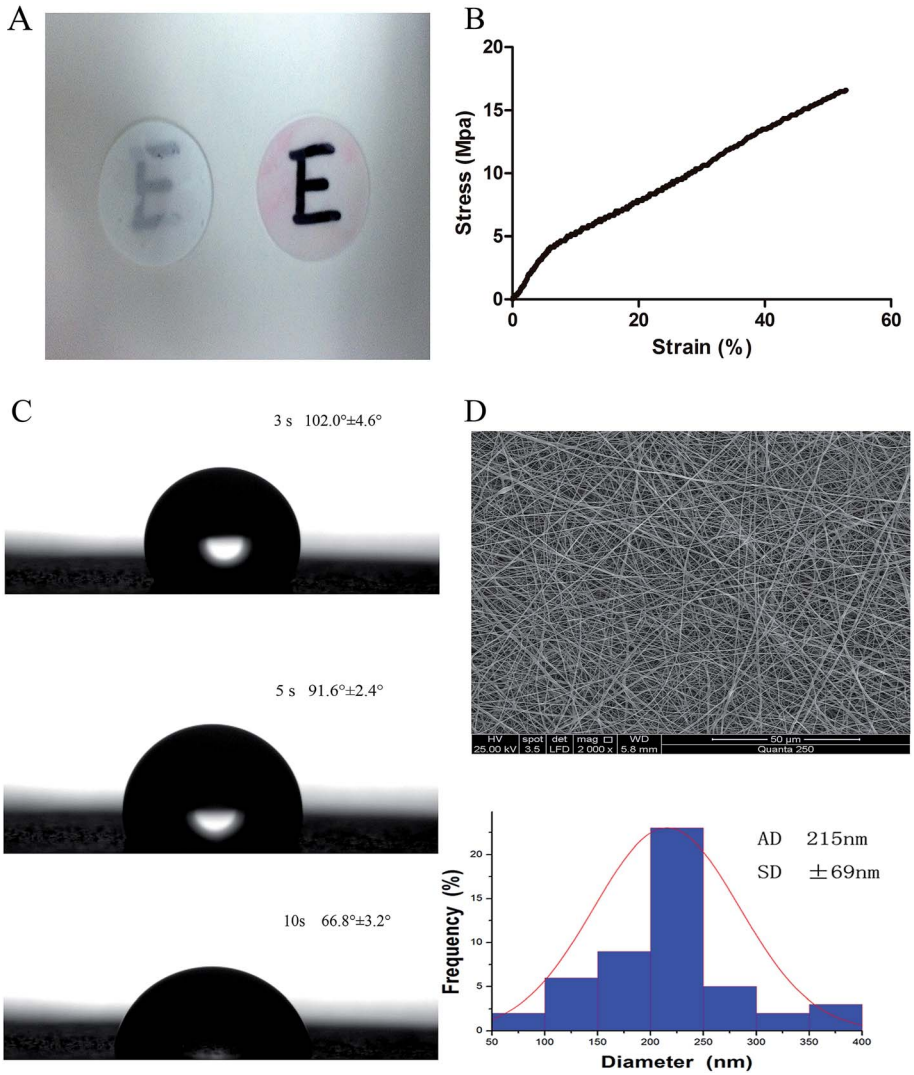

Fig. 1 Characterization of SF/PLCL scaffolds. (A) Transparency of SF/PLCL scaffolds before and after immersion in cell culture media. (B) Mechanical properties of SF/PLCL scaffolds. (C) Water contact angles of SF/PLCL scaffolds at different times. (D) SEM image and diameter distribution of SF/PLCL scaffolds.

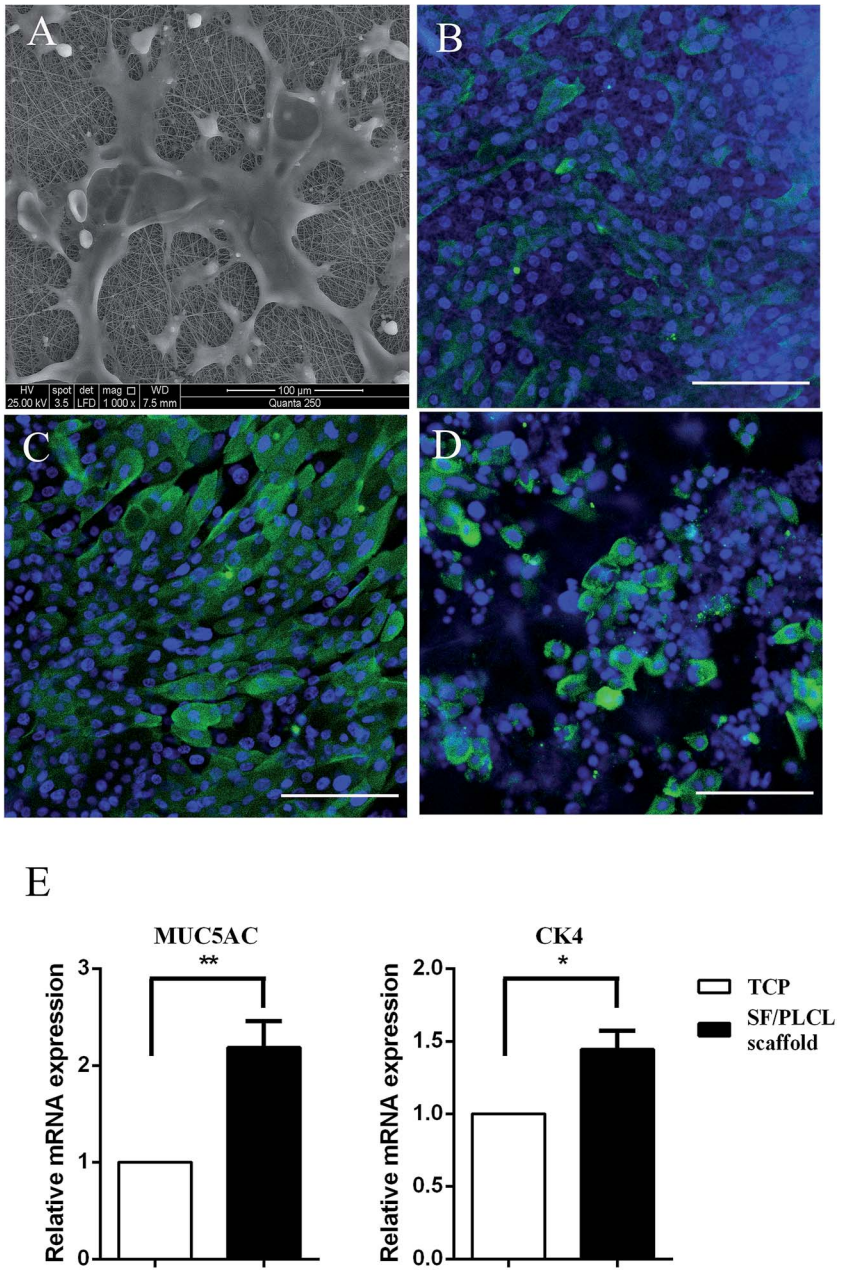

Fig. 2 Morphology and phenotypes of CjECs on SF/PLCL scaffolds. (A) Morphology of CjECs after culturing for 2 days. Immunocytochemistry was performed to visualize conjunctival epithelial specific markers: (B) CK4 for epithelial cells, (C) CK19 for epithelial cells, and (D) MUC5AC for goblet cells. (E) qPCR analysis of the expression of conjunctival epithelial specific genes. *$p < 0.05$, **$p < 0.01$. Scale bars: 100 μm.

a 1.4- and 2- fold increase in CK4 and MUC5AC transcripts respectively, in comparison to those cultured on TCPS (Fig. 2E).

Viability and proliferation of conjunctival epithelial cells *in vitro*

The Live/Dead staining analysis showed that a few dead cells grown on the scaffolds, which were stained red, could be seen, with no significant differences from the TCPS group, indicating that the scaffolds were nontoxic to the CjEC cultures (Fig. 3A).

To determine the effect of the scaffolds in supporting cell growth, we seeded CjECs on the scaffolds and measured the cell proliferation abilities using BrdU staining and the CCK-8 assay. Immunocytochemistry analysis showed that the cells on SF/PLCL scaffolds stained positively for BrdU, a cellular marker for proliferation (Fig. 3B). As shown in Fig. 3C, the CCK-8 assay demonstrated that the cells proliferated well and the number of the cells increased in a time dependent manner.

Conjunctival epithelial cells combined with SF/PLCL scaffolds induced no upregulation of interleukin 6 (IL-6) expression

To investigate whether the scaffolds would elicit elevated expression of inflammatory genes, the expression level of the IL-

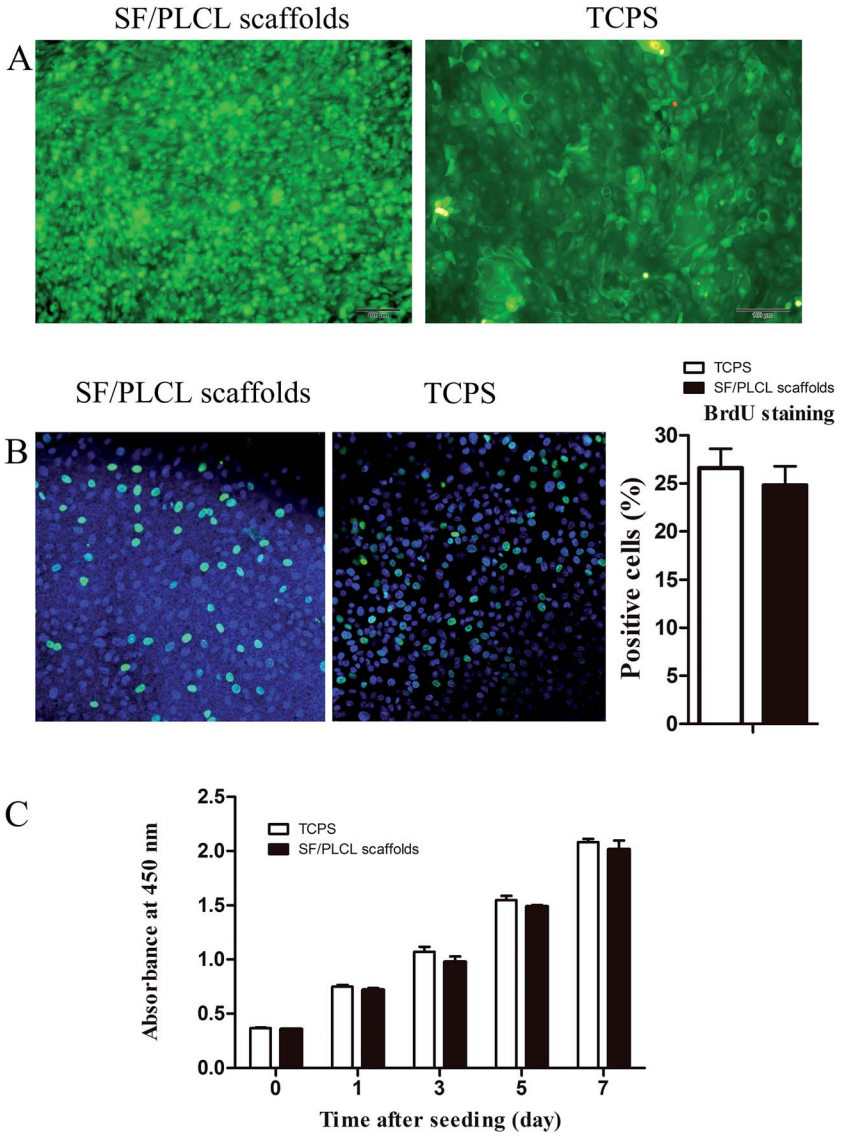

Fig. 3 Effects of SF/PLCL scaffolds on CjEC viability and proliferation. (A) Live (green)/Dead (red) staining of CjECs on SF/PLCL scaffolds and TCPS. (B) BrdU staining of CjECs on SF/PLCL scaffolds and TCPS. (C) CCK-8 analysis of the proliferation of CjECs on SF/PLCL scaffolds and TCPS. Scale bars: 100 μm.

6 gene was analyzed by qPCR after different times of culturing. We demonstrated that there was no statistically significant difference in IL-6 expression of CjECs grown on SF/PLCL scaffolds and TCPS (Fig. 4), suggesting that SF/PLCL scaffolds might not elicit obvious inflammatory responses for conjunctiva reconstruction.

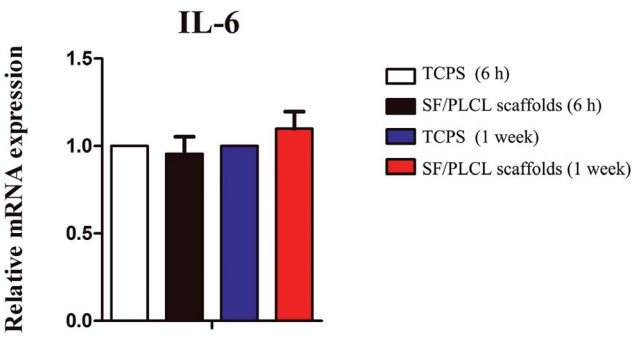

Fig. 4 qPCR analysis of IL-6 gene expression after cells were seeded on SF/PLCL scaffolds for 6 h and 1 week. qPCR analysis of IL-6 gene expression after CjECs were seeded on SF/PLCL scaffolds at different time points.

Histological and immunohistochemical analysis of conjunctival epithelial cells cultured on SF/PLCL scaffolds *in vitro* and *in vivo*

After culturing for 1 week *in vitro*, the CjECs generated an epithelium 2–4 layers thick as observed on H&E stained sections (Fig. 5A).

To evaluate the biocompatibility of SF/PLCL scaffolds, H&E and MUC5AC staining was performed. MUC5AC staining

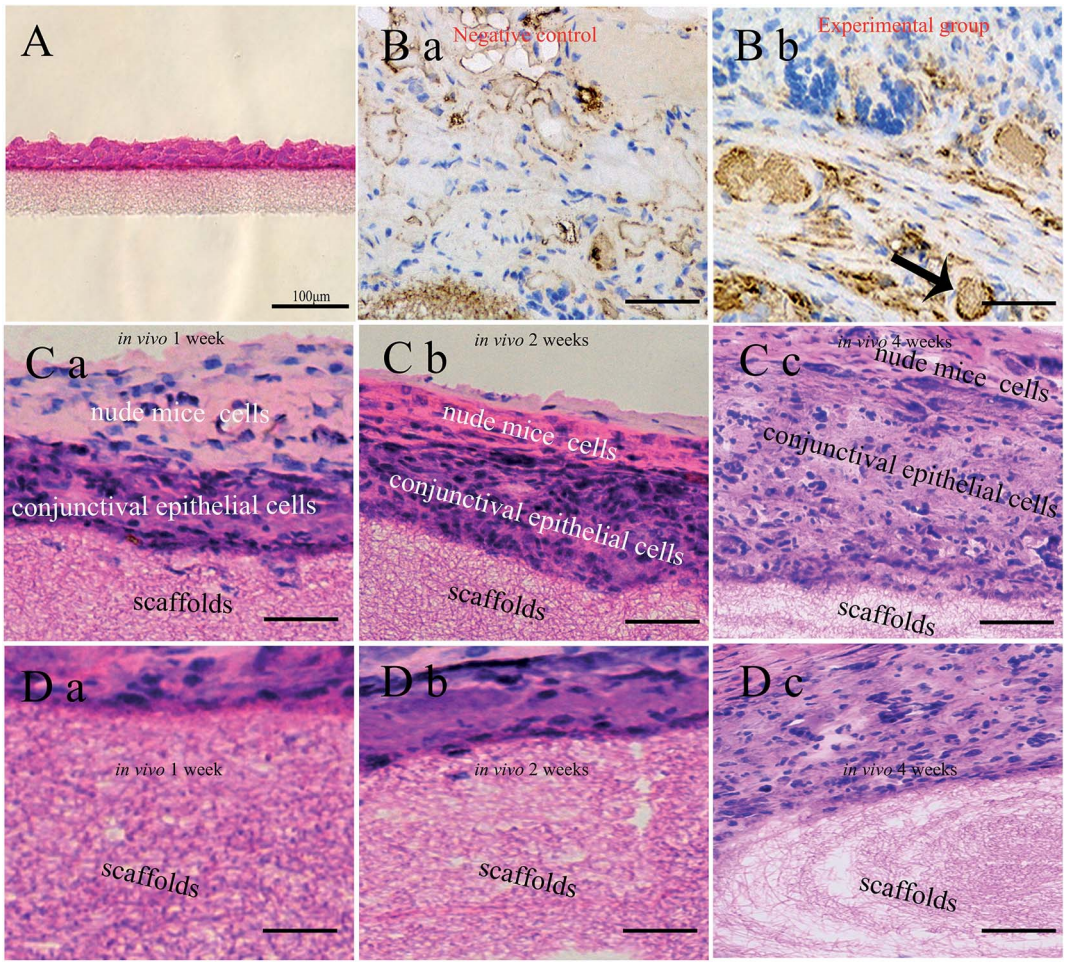

Fig. 5 Histological staining of the cell-seeded scaffolds *in vitro* and *in vivo*. (A) H&E staining of the stratification of CjECs on SF/PLCL scaffolds after culturing for 1 week *in vitro*. (B) MUC5AC staining was used to visualize goblet cells (arrowhead: goblet cells). Histological images of cell-seeded scaffolds *in vivo* with H&E staining at different time points, (C) the stratification of CjECs, and (D) the degradation of the scaffold nanofibers. Scale bars: 100 μm.

showed that goblet cells that occurred singly or in clusters were present among the stratified epithelial cells (Fig. 5B). The results of H&E staining showed that with the extension of implantation time *in vivo*, CjECs formed more and more stratification structures, and meanwhile, the fibers of the scaffolds gradually degraded (Fig. 5C, D).

Discussion

The conjunctiva is an important functional and structural component of the ocular surface, and the conjunctival epithelium secrets the mucin component of the tear film and protects the ocular surface.[28] Conjunctiva-related diseases and injuries will compromise the homeostasis and functionality of the ocular surface. In severe cases, tissue-engineering strategies could be applied for optimal reconstruction to prevent fibrosis and wound contracture, especially symblepharon.[8] A ideal scaffold used in conjunctiva engineering should exhibit the following properties: biocompatibility and biodegradability for cell attachment and proliferation, with a well-interconnected pore network to allow the transport of nutrients and metabolic waste, and ability to be well tolerated without causing inflammation or stimulating rejection. Importantly, the scaffolds should also preserve the physiological CjEC features *in vivo*, such as the phenotypic development containing distinctive goblet cells.[29,30] Our previous results on the wettability of the scaffold showed that the pure PLCL scaffold was hydrophobic, whereas the incorporation of SF dramatically lowered the contact angle of the SF/PLCL scaffolds. The water contact angle of the SF/PLCL (75/25) scaffold was 66.8° ± 3.2°, which is in the range of favorable water contact angles (water contact angle 50–70°) for cell attachment and proliferation. Last but not least, our previous study demonstrated that SF/PLCL scaffolds were porous nanofibrous scaffolds with high porosity and a high surface area resembling the topographic features of the ECM, to which the structure contributed nutrients and gas exchange, cell attachment and proliferation. In this study, SEM showed that the average fiber diameter of the SF/PLCL (75/25) scaffold was 215 nm ± 69 nm, which demonstrated that the average fiber diameter of around 200 nm could better promote cell attachment, proliferation, and migration.[20,31]

One of the most important hallmarks of the conjunctival epithelium is the goblet cells that synthesize, store and release MUC5AC.[25,32,33] Many ocular surface defects are accompanied by goblet cell loss and/or mucin component alteration.[34] Therefore, the functional restoration of goblet cells may be a critical procedure for the reconstruction of the ocular surface. Previously, it was commonly accepted that a conjunctival epithelium cultivated *in vitro* can hardly develop the goblet cell phenotype.[35] However, our results showed that SF/PLCL scaffolds supported the growth and phenotypic development of goblet cells. We speculate that the advantageous effect of SF/PLCL scaffolds in supporting differentiation of goblet cells could be attributed to its electrospun fibrillar structure, which closely mimics the structure and function of the ECM, because the highly porous structure of interconnected pores provides proteins, genes, nutrients and gas exchange.

Few previous studies examined whether the biomaterials could affect the secretion of pro-inflammatory factors by CjECs. IL-6, one of the most important molecules in conjunctival inflammation, was analyzed by qPCR.[2,36] The results showed that at different culture times of CjECs, there was no significant difference in IL-6 expression, indicating that SF/PLCL scaffolds might not elicit obvious inflammatory responses for conjunctival reconstruction.

We also evaluated the formation *in vitro* and *in vivo* of conjunctiva tissue by seeding CjECs on the scaffolds. *In vitro* CjECs cultured on the scaffolds generated an epithelium 2–4 layers thick. With the extension of implantation time *in vivo*, the CjECs formed more and more stratification structures as observed using H&E staining. It has been reported that degradation properties play a pivotal role in the selection and design of the biomaterials. The ideal degradation speed of the scaffold should match the rate of conjunctival regeneration.[37] H&E staining showed that with the extension of the implantation time *in vivo*, the fibers of the scaffolds gradually degrade, and the degradation products of SF/PLCL scaffolds are amino acids from SF, and lactic acid and caproic acid from PLCL, and these are metabolizable and nontoxic.[38] Thus, these findings indicate that SF/PLCL scaffolds could promote conjunctiva formation.

Conclusions

SF/PLCL scaffolds, with high porosity and high surface area resembling the topographic features of the ECM, were successfully prepared using electrospinning techniques. Our data demonstrated that SF/PLCL scaffolds not only promoted CjEC growth and proliferation without any inflammatory reaction, but also maintained the phenotypic development of CjECs. Moreover, CjECs cultured on the scaffolds could form a stratified conjunctival epithelium including goblet cells, suggesting that SF/PLCL scaffolds may be preferable for conjunctival regeneration.

Conflicts of interest

The authors declare that no competing financial interests exist.

Acknowledgements

The authors are grateful for the assistance of Mo Xiumei of Donghua University (Shanghai, China). The study was supported by the National Natural Science Foundation of China (no. 81370992, 81570812, and 81500765), the Shanghai Municipal Education Commission: Gaofeng Clinical Medicine Grant Support (grant no. 20161421), the Shanghai Municipal Science and Technology Commission: the Commercialization and Industrialization of Research Findings Project (grant no. 17411963800) and The Science and Technology Commission of Shanghai (17DZ2260100).

References

1 I. K. Gipson, *Invest. Ophthalmol. Visual Sci.*, 2007, **48**(4390), 4391–4398.
2 L. Garcia-Posadas, I. Arranz-Valsero, A. Lopez-Garcia, L. Soriano-Romani and Y. Diebold, *Invest. Ophthalmol. Visual Sci.*, 2013, **54**, 7143–7152.
3 S. Selvam, P. B. Thomas and S. C. Yiu, *Ocul. Surf.*, 2006, **4**, 120–136.
4 H. Zhan, H. M. Towler and V. L. Calder, *Invest. Ophthalmol. Visual Sci.*, 2003, **44**, 3906–3910.
5 W. Li, X. Sun, Z. Wang, R. Li and L. Li, *Mol. Vision*, 2010, **16**, 2739–2744.
6 M. P. Hatton and P. A. Rubin, *Adv. Biochem. Eng./Biotechnol.*, 2005, **94**, 125–140.
7 S. Schrader, M. Notara, M. Beaconsfield, S. J. Tuft, J. T. Daniels and G. Geerling, *Curr. Eye Res.*, 2009, **34**, 913–924.
8 J. R. Eidet, I. G. Fostad, M. A. Shatos, T. P. Utheim, O. A. Utheim, S. Raeder and D. A. Dartt, *Invest. Ophthalmol. Visual Sci.*, 2012, **53**, 2897–2903.
9 S. Khalili, S. Nouri Khorasani, M. Razavi, B. Hashemi Beni, F. Heydari and A. Tamayol, *J. Biomed. Mater. Res., Part A*, 2018, **106**(2), 370–376.
10 J. Ye, X. Shi, X. Chen, J. Xie, C. Wang, K. Yao, C. Gao and Z. Gou, *J. Mater. Chem. B*, 2014, **2**, 4226–4236.
11 S. W. Choi, Y. Zhang and Y. Xia, *Langmuir*, 2010, **26**, 19001–19006.
12 K. Zhang, H. Wang, C. Huang, Y. Su, X. Mo and Y. Ikada, *J. Biomed. Mater. Res.*, 2010, **93**, 984–993.
13 W. Fu, Z. Liu, B. Feng, R. Hu, X. He, H. Wang, M. Yin, H. Huang, H. Zhang and W. Wang, *Int. J. Nanomed.*, 2014, **9**, 2335–2344.
14 A. R. Murphy, P. St John and D. L. Kaplan, *Biomaterials*, 2008, **29**, 2829–2838.
15 R. You, Y. Xu, Y. Liu, X. Li and M. Li, *Biomed. Mater.*, 2014, **10**, 015003.
16 V. P. Ribeiro, A. da Silva Morais, F. R. Maia, R. F. Canadas, J. B. Costa, A. L. Oliveira, J. M. Oliveira and R. L. Reis, *Acta Biomater.*, 2018, **72**, 167–181.
17 I. K. Kwon, S. Kidoaki and T. Matsuda, *Biomaterials*, 2005, **26**, 3929–3939.
18 C. Y. Xu, R. Inai, M. Kotaki and S. Ramakrishna, *Biomaterials*, 2004, **25**, 877–886.

19 B. S. Kim and D. J. Mooney, *Trends Biotechnol.*, 1998, **16**, 224–230.
20 Z. Wang, M. Lin, Q. Xie, H. Sun, Y. Huang, D. Zhang, Z. Yu, X. Bi, J. Chen, J. Wang, W. Shi, P. Gu and X. Fan, *Int. J. Nanomed.*, 2016, **11**, 1483–1500.
21 D. Zhang, N. Ni, J. Chen, Q. Yao, B. Shen, Y. Zhang, M. Zhu, Z. Wang, J. Ruan, J. Wang, X. Mo, W. Shi, J. Ji, X. Fan and P. Gu, *Sci. Rep.*, 2015, **5**, 14326.
22 J. Chen, C. Yan, M. Zhu, Q. Yao, C. Shao, W. Lu, J. Wang, X. Mo, P. Gu, Y. Fu and X. Fan, *Int. J. Nanomed.*, 2015, **10**, 3337–3350.
23 L. Chen, Y. Bai, G. Liao, E. Peng, B. Wu, Y. Wang, X. Zeng and X. Xie, *PLoS One*, 2013, **8**, e71265.
24 Q. Yao, M. Zhu, J. Chen, C. Shao, C. Yan, Z. Wang, X. Fan, P. Gu and Y. Fu, *Mol. Vision*, 2015, **21**, 1113–1121.
25 J. R. Eidet, O. A. Utheim, S. Raeder, D. A. Dartt, T. Lyberg, E. Carreras, T. T. Huynh, E. B. Messelt, W. E. Louch, B. Roald and T. P. Utheim, *Exp. Eye Res.*, 2012, **94**, 109–116.
26 M. W. Pfaffl, *NucleicAcids Res.*, 2001, **29**, e45.
27 R. Nakajima, T. Kobayashi, T. Kikuchi, Y. Kitano, H. Watanabe, M. Mizutani, T. Nozaki, N. Senda, K. Saitoh, R. Takagi, M. Yamato, T. Okano and S. Takeda, *J. Tissue Eng. Regener. Med.*, 2015, **9**, 637–640.
28 L. Su, H. Cui, C. Xu, X. Xie, Q. Chen and X. Gao, *Curr. Eye Res.*, 2011, **36**, 797–803.
29 Q. L. Loh and C. Choong, *Tissue Eng., Part B*, 2013, **19**, 485–502.
30 P. Xiang, K. C. Wu, Y. Zhu, L. Xiang, C. Li, D. L. Chen, F. Chen, G. Xu, A. Wang, M. Li and Z. B. Jin, *Biomaterials*, 2014, **35**, 9777–9788.
31 G. T. Christopherson, H. Song and H. Q. Mao, *Biomaterials*, 2009, **30**, 556–564.
32 L. Tian, M. Qu, Y. Wang, H. Duan, G. Di, L. Xie and Q. Zhou, *Exp. Eye Res.*, 2014, **123**, 37–42.
33 F. L. Barbosa, Y. Xiao, F. Bian, T. G. Coursey, B. Y. Ko, H. Clevers, C. S. de Paiva and S. C. Pflugfelder, *Int. J. Mol. Sci.*, 2017, **18**(5), 978.
34 M. Dogru, N. Okada, N. Asano-Kato, M. Tanaka, A. Igarashi, Y. Takano, K. Fukagawa, J. Shimazaki, K. Tsubota and H. Fujishima, *Cornea*, 2005, **24**, S18–S23.
35 H. Zhou, Q. Lu, Q. Guo, J. Chae, X. Fan, J. H. Elisseeff and M. P. Grant, *Biomaterials*, 2014, **35**, 7398–7406.
36 A. Enriquez-de-Salamanca, V. Calder, J. Gao, G. Galatowicz, C. Garcia-Vazquez, I. Fernandez, M. E. Stern, Y. Diebold and M. Calonge, *Cytokine*, 2008, **44**, 160–167.
37 R. Murugan and S. Ramakrishna, *Tissue Eng.*, 2007, **13**, 1845–1866.
38 R. Rosario-Melendez, L. Lavelle, S. Bodnar, F. Halperin, I. Harper, J. Griffin and K. E. Uhrich, *Polym. Degrad. Stab.*, 2011, **96**, 1625–1630.